Journal of Information Systems Engineering and Management
2025, 10(3s)
e-ISSN: 2468-4376
https://www.jisem-journal.com/

Research Article

Management of Construction, Stability, and Performance in Solar-Powered Metal Halide Photo-Catalysis Systems

Prof. Deageon Kim[1], Prof. Dongoun Lee[2]
[1]*Department of Architectural & Civil Engineering, Dongseo University, 47, Jurye-ro, Sasang-gu, Busan, Republic of Korea*
ORCID: 0000-0002-4000-2225
[2]*Department of Architectural & Civil Engineering, Dongseo University, 47, Jurye-ro, Sasang-gu, Busan, Republic of Korea*
ORCID: 0000-0002-9158-304X
Corresponding Author: Prof. Deageon Kim

ARTICLE INFO

Received: 04 Oct 2024
Revised: 08 Dec 2024
Accepted: 19 Dec 2024

ABSTRACT

The formation of harmless to the ecosystem, monetarily reasonable, and chemically efficient cycles is the present key chemistry challenge. Presently, semiconductor heterogeneous photocatalysis is utilized in many cycles that affect society, from those that produce hydrogen and convert CO2 to those that transform natural unrefined substances into compounds with added esteem. Metal halide perovskites have recently emerged as a possible inspirational class of unassuming and simple to create photocatalytic semiconductors, despite their precariously abruptly supported gem structure. However, up until now, their widespread use has been required. We examine the challenges MHP-based photocatalysis encounters in this Review and emphasize the numerous frameworks being employed to create circumstances that are both favourable and stable for photocatalytic reaction. For hydrogen development responses, we explicitly talk about the utilization of (1) halogen corrosive arrangements (HX; X = I or Br), (2) extremely low-extremity solvents for natural changes and CO2 photograph decrease, and (3) the embodiment of perovskites for CO2 decrease and water parting. The means used to make innately stable photocatalytic materials are additionally definite, eliminating the interest for uncommon conditions. We close by introducing possibly alluring open doors and approaches for metal halide perovskite-based photocatalysis research going ahead, with every innovation offering particular arrangements of benefits and challenges.

Keywords: MHP, Solar energy, Photo-catalysis, Stability, Performance

INTRODUCTION

Like the proficient and normal energy change showed by photosynthesis, photocatalysis offers a fruitful technique for counterfeit sunlight based to-compound energy transformation (Kim et al., 2015; Kamat, 2007). The 1972 publication of a UV-driven photocatalytic hydrogen mix on TiO2 (Fujishima & Honda, 1972) ignited many years of logical innovative work that have brought about various pivotal applications for human culture, including energy change, (for example, water parting and CO2 decrease) and substance changes as well as the expulsion of natural toxins. The three fundamental cycles that photocatalytic materials use to drive responses are I photon retention to create electron and opening matches, (ii) charge detachment and growth to response zones on the photocatalysts surface; and (ii) compound oxidation and decreasing at the surface, autonomously, which are interceded by the photograph conveyed openings and electrons (Hisatomi et al., 2014). A few helpful actual qualities, including solid and expansive light retention, powerful charge detachment, long working dependability, and the right redoX capacity for target responses, need be available in a photocatalytic material for it to be ideal (Ge et al., 2017). Nonetheless, most of photocatalysts are nowhere near great. Unaltered TiO2, graphitic carbon nitride (g-C3N4), and BiVO4 are a few examples of materials with drawbacks, an expansive bandgap (Wen et al., 2017), a high pace of photograph produced charge transporter recombination, and a low photograph decrease potential (He et al., 2014). This implies that broad material revelation and examination inside the discipline is as yet determined by a powerful urge to make novel semiconductor photocatalysts with satisfactory characteristics.

Copyright © 2024 by Author/s and Licensed by JISEM. This is an open access article distributed under the Creative Commons Attribution License which permitsunrestricted use, distribution, and reproduction in any medium, provided the original work is properly cited.

Continuous upgrades in useful sun arranged cells; LEDs, lasers, and photodetector advancement have made metal halide perovskite semiconductors look charming as optoelectronic materials (Ha et al., 2017). MHPs' productive use in optoelectronic contraptions is essentially fueled by their affordable gathering and clear plan taking care of (Brenner et al., 2016); tunable direct bandgap (Mosconi et al., 201323, (Herz, 2016); broad carrier scattering lengths (Wehrenfennig et al., 2014); high carrier adaptability (Jin et al., 2020) and unusually high carrier convenience (Park et al., 2017).

As seen in Figure 1, MHPs have very narrow bandgap energies when compared to more conventional photocatalysts, allowing them to absorb solar photons with lesser energy.

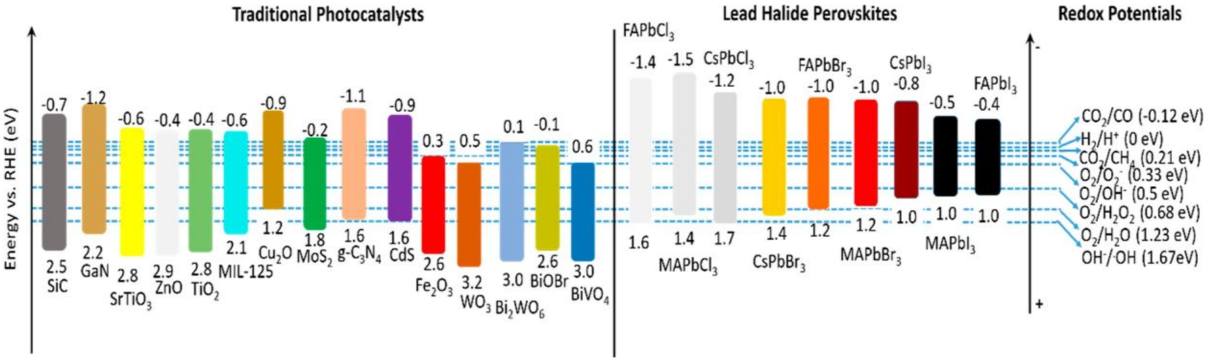

Figure 1: Band edge locations of various MHPs and conventional photocatalysts

Several MHPs and conventional photocatalysts' band edge positions are determined by the RHE (reversible hydrogen anode) (Wen et al., 2017; He et al., 2014; Elumalai et al., 2016; Wu et al., 2018; Tamirat et al., 2016; Hendon et al., 2013; Jiang et al., 2018; Kibria & Mi, 2016; Wang et al., 2019; Xie et al., 2016, Wu et al., 2018). A few frequent half-response' redox capabilities are also demonstrated for correlation (Xiao et al., 2013; Kong et al., 2018; Li et al., 2016; Stranks et al., 2015).

The electronic band design of a semi-director should coordinate the response redoX expected as per response thermodynamics. Figure 1, showcases the possibilities of common photocatalytic half-responses connected with color debasement, CO2 decrease, water parting, and vigorous natural change. Additionally, this image displays the generic MHP valence band and conduction band positions. Figure 1 represents the predominant decrease capacity of MHPs in view of their correlation; explicitly, the overall place of their CB is much of the time adequately negative for H2 age, CO2 decrease, and superoxide revolutionary creation. Furthermore, some MHP relatives can theoretically in like manner achieve water cleansing as a result of their more certain valence band maxima, oxidation (VBM). The required potential for hydroxyl revolutionary creation, which is every now and again engaged with color corruption, is higher than the VBM of MHPs, barring them as competitors.

Given the (photograph) actual qualities showed by MHPs, they seem to meet various critical measures for viable photocatalytic processes, as portrayed in Figure 1. As a matter of fact, the principal concentrate on MHP-based photocatalysis was distributed in December 2016, when Nam and collaborators (Quan et al., 2018) depicted a technique for photocatalytically driving Howdy parting with MAPbI3 by exploiting the unique balance of MAPbI3 disintegration and reprecipitation in soaked Hey watery arrangements. The ionic cross section of MHPs is very unsteady under more normal photocatalytic response conditions, thus this specific technique functioned admirably. For example, water or a polar dissolvable is fundamental for H2O parting, CO2 and N2 decrease, and color corruption, which advance debasement pathways that are all unsafe for long haul utilization (Figure 2) (Wang et al., 2019; Yang, et al., 2015). The ongoing prospects of effectively involving MHPs in photocatalysis are investigated in this survey. We offer a basic evaluation of the unsteadiness issues blocking improvement in this fresh out of the box new area of logical review and feature dependable strategies advancing stable response conditions. The future issues and chances of this astonishing new innovation are momentarily talked about in the last segment.

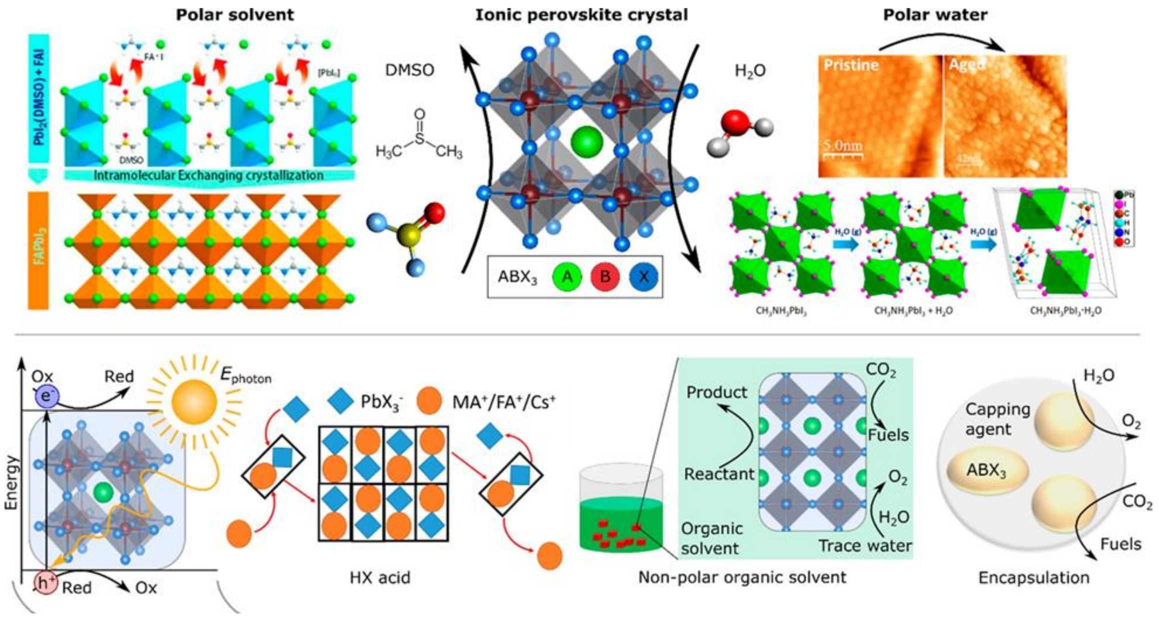

Figure 2: Approaches toward stable photocatalytic reaction environments

Top: An example of how MHP surfaces can become vulnerable to polar solvents (like DMSO) and water during photocatalytic processes. Polar molecules quickly interchange intramolecularly with the organic cation, which results in the instantaneous breakdown of the perovskite's chemical composition (Zhu et al., 2016; Murali et al., 2016; Takata & Domen, 2019). A monohydrate perovskite structure is created as a result of the stepwise destruction of MHPs by water molecules. This structure later degrades into nonperovskite structures via various stages. When using MHPs as a photocatalyst, there are three main ways to create stable reaction environments: epitome by means of covering specialists or shelling forestalls direct contact with polar solvents or response items; nonpolar or moderately low-extremity dissolvable scattering diminishes the corruption pathways; and soaked haloacid arrangements balance out MHPs by laying out a powerful ionic harmony between the broke down ionic species and the strong perovskites.

LITERATURE REVIEW

2.1 Photocatalysis using particles in suspension

The following specific processes make up the semiconductor-based photocatalytic process in general. These incorporate the accompanying: engrossing sunlight based light, delivering photograph energized electrons and openings, isolating the made electron-opening pair, moving the created electrons and openings to the outer layer of photocatalysts (responsive locales), and photocatalytic responses occurring at the receptive destinations. Upgraded photocatalytic transformation proficiency results from the photocatalytic frameworks that help these cycles.

In the wake of being presented to light, the semiconductor goes about as a photocatalysts in a framework for photocatalysis by suspended particles and produces charge transporters. Knowing the reasonable differentiation (Eo) licenses one to calculate the most diminished recurrence of the photon that can cause excitation. The standard Gibb's free energy change (Go) of the responses is utilized to get the worth of Eo. The "Go" an incentive for decrease of CO2 into CO is 259 kJ/mol, while the "Go" an incentive for H2O parting (H2OH2 1/2O2) is 237 kJ/mol. These numbers relate to bandgaps of 1.23 and 1.34 eV, separately (Go Eo) (Qian et al., 2019).

For the excitation of charge transporters that can drive the reduction of CO2 and the isolation of water, freely varying radiations with frequencies of 1007 nm and 956 nm are typical. As a result, UV and NIR light frequencies are sufficient to power the cycle for the progress of created fuel. After the semiconductor is acquainted with light, the charge transporters that are taken their action to the responsive districts and begin the redoX cycle. Considering its optoelectronic qualities, like a tremendous dispersing length, and so on, XP limits the chance of charge transporter recombination. The electron's potential must be higher in the negative for decrease reactions and higher in the positive for oxidation reactions for the photocatalytic reactions to take place. The debate between charge transporter recombination and the ideal response on a shallow level is the essential determinant of photocatalytic feasibility. The semiconductor contact is one more conceivable district for the recombination. More cautionary information regarding the charge age and transport in a semiconductor can be found in the study by Qian et al. (2019).

Higher dissemination length and tunable bandgaps in XP materials bring about lower recombination (Lin et al., 2016; Lee et al., 2012; Xing et al., 2013; Wang et al., 2016). Due to the more noteworthy bandgap of the perovskite materials, the delivered electron and opening have the fundamental potential to cause CO2 decrease and water dividing responses.

In the genuine trial technique, active command over the cycle is likewise important to successfully use the electrons and openings produced notwithstanding the thermodynamic rules recently examined. As a rule, co-impetuses like Pt, MoS2, and RuO2 are expected to increment synergist productivity. We go over the suspended molecule photocatalyst frameworks for CO2 decrease and H2 development independently in the subsections that follow.

2.2 MHP structure and characteristics

A famous equation for the MHP semiconductor family is ABX3, which utilizes the gem construction of calcium titanate (CaTiO3). A site of MHPs can regularly integrate various cations (normal or inorganic), a metal cation has the B position, and X is a halide anion (Suarez et al., 2014). MHPs have uncommon photoelectronic properties considering their ionic valuable stone and semiconducting characteristics. The bandgap of MAPbX3 can be efficiently modified by altering the kind or molar degree of the halides on the X site (Green et al., 2014). Because of the Pb-concluded p electrical transitions from the valence band to the conduction band, symmetric turn of events, and direct bandgap, MAPbI3 has a high optical support coefficient (Dong et al., 2015). MHPs have an extensive transporter dissemination length that can arrive at north of 100 m for a solitary precious stone because of their deformity resistance qualities (Giorgi et al., 2013). Moreover, due of the low exciton restricting energy in MAPbI3, photograph energized charge transporters move like free transporters and ambipolar transporter portability with indistinguishable compelling masses for electrons and openings (Quilettes et al., 2015; Xiao et al., 2019). The upsides of MHPs for photocatalytic applications will be featured alongside the photocatalytic interaction due to their uncommon photoelectronic capacities.

When the band-structure theory is taken into account, the photocatalytic cycle can be separated into three major phases, including (a) light support, (b) charge package and move, and (c) redox responses. (Park & Segawa, 2018). only photons with energy bigger than the bandgap of semiconductors can strengthen electrons from the VB to the CB when illuminated by light sources. An additional degree of the sun-based reach can be transformed into charge carriers at night when the bandgap is smaller. For instance, a 1.6 eV bandgap perovskite's speculative PCE limit is 30.14%. (Guo et al., 2019). A higher efficiency of MHPPs is anticipated because to the successfully adjusted bandgap and reliable optical ingestion coefficient of MHPs. Charge recombination took place between 1015 and 106 seconds after the photo induced excitons to split into electrons and openings and travel to dynamic areas (Zhou et al., 2021). The large number of tenants in charge transporters that attend active protests is a result of MHPs' low exciton holding energy, high transporter movability, long charge dispersal length, and covered charge recombination. Finally, in active regions, charge carriers that have attained sufficiency should end redox processes. The mechanisms leading to the reduction in water and CO2 start when the CB maximums of MHPs are sufficiently negative. The utilization of charge carriers is constrained by the slow reaction rate (106 s to 103) of MHP absconds, which might act as strong districts to lower the energy barrier and speed up redox processes. Due to the fact that photoactive materials used in both photovoltaics and photocatalysis share several similar systems of light support, charge partition, and movement, the remarkable electronic and optical properties of MHPs convey high PCE for photovoltaic applications as well as demonstrate a (high potential for use in those processes.

METHODOLOGIES

3.1 MHP Photocatalyst Instability:

The basic and optoelectronic properties of MHPs are influenced by stage changes, temperature stress, receptivity to integrating air (oxygen and clamminess), and illumination throughout (UV light). Exactly when in contact with polar added substances, the charged pieces of MHP diamonds are helpless against basic changes near the surface in view of the ionic affiliations that difficult situation them (Kwon et al., 2014). The confined degree of photocatalytic responses for which these semiconductors have been truly utilized is depicted by this particular characteristic of MHPs. Figure 2 demonstrates how MHPs open to polar particles and as frequently as possible separate into a PbX (X = I, Br, Cl) prMA/FA cation and halide anion. Cross variety regular inorganic MHPs' MA+ and FA+ cations, which are capricious hygroscopic amine salts, cause clamminess insecurity. (Christians et al., 2015). A polycrystalline nonperovskite essential covering and grain limits are made in view of water's collaboration with the diamond through hydrogen holding in Figure 2. The quantitative and accurate evaluation of the sogginess-induced essential and engineered corruption part of MAPbI3 has been carried out using stomach muscle initio sub-nuclear components entertainments, ultrafast transient maintenance spectroscopy and energy studies, (Mosconi et al., 2015) in situ brushing event X-shaft diffraction, and in situ contacting rate X-pillar diffraction (Huang et al., 2017). The [PbX6]4 octahedral units of the MHPs answer with the held water particles to make widely appealing monohydrate and dihydrate structures. Speedy material breakdowns through hydrolyzation follow this (eqs 1–2): (Schneider & Bahnemann, 2013).

$CH_3NH_3PbI_3{\cdot}H_2O \rightarrow PbI_2 + CH_3NH_3I + H_2O$ (1)

$CH_3NH_3I \rightarrow CH_3NH_2 + HI$ (2)

Water produces two new kinds of hydrogen bonds, major areas of strength for one with the grid halides and the other feebly with the natural cations; As a result of interfering with the hydrogen connection between the organic and inorganic units, it threatens the stability of the perovskite structure (Yang et al., 2015). Outstandingly, it is just at the monohydrate stage change, when the two become locked, that the cooperation among Mama and H2O is laid out. (Zhu et al., 2016) Because of the fast development of water particles across grain limits in polycrystalline flimsy movies, the monohydrate stage advancement happens no matter what the film thickness.

3.2 Saturated Haloacid Solutions:

Because MHPs are water-dissolvable ionic mixtures, one innovative approach to the problem of reliable quality is to leverage the precipitation-dissolvability balance between the perovskite stage and the dissolvable ionic species. Using MAPbI3 perovskite polycrystalline powders, Nam et al. first shown the photocatalytic H2 ageing in the horrible watery game-plan of methylammonium lead iodide (MAPbI3) drenched hydrogen iodide (Great news). MAPbI3 particles of micrometer size separate in a splashed Welcome response for creating PbIx complex anions and methylammonium cations. As shown in Figures 3A and 3B, while an equivalent number of these particles moreover recrystallizes. The (I) and H+ molecule centers in the watery game plan would have a basic impact in controlling the MAPbI3 stage. The MAPbI3 perovskite continuously ease remained stable in an arrangement of fairly high molecule obsession (>3.16 mol/L Welcome game plan), alongside a reduced iodide center. The response pathway for photocatalytic Hello parting on MAPbI3 is displayed in Figure 3C. These blends involved MAPbI3 as a photocatalyst to create around 26 mol of H2 in 9 hours when presented to noticeable light (475 nm). H3PO2 was also added to keep up with the I-fixation since it is a powerful diminishing specialist of I3 to I. Because of the powerful harmony between the ionic species in the immersed arrangement and the MAPbI3 powders, MAPbI3 stayed stable for 160 hours under consistent illumination without encountering any action split the difference, as displayed in Figure 3D. The hydrogen development rate was likewise further developed by the Pt testimony on the MAPbI3 (i.e., Pt/MAPbI3), arriving at 57 mol/g/h, yielding a sun based to-substance transformation productivity (the extent of sun oriented radiation changed to compound energy) of 0.81%.

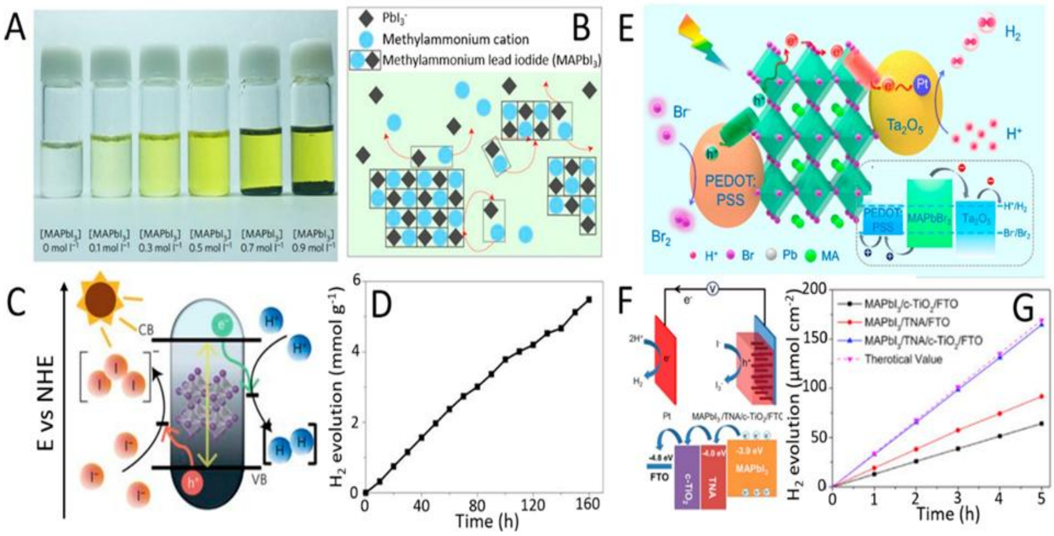

Figure 3: MAPbI3 particles of micrometer size separate in a splashed

In above figure (A) For the good news isolating photocatalytic response, a band contour of the MAPbI3 powder, (B) For the friendliness between the decay and recrystallization of MAPbI3 in a lowered Howdy plan, (C) a stable photocatalytic H2 improvement in the soaking solution for 160 hours. (E) MAPbBr3 and Pt/Ta2O5 are used as the electron- and opening moving subject in a photocatalytic HBr isolating response device. (F) Charge move plan, and (G) H2 improvement.

These reassuring cases show that soaked watery halogen corrosive arrangements give a fitting response media to MHP-based photocatalytic hydrogen development, as itemized in Table 1. MHPs keep up with their dependability in the immersed HX corrosive arrangement because of the precipitation-dissolvability balance. The energetics of the photocatalyst structure might be controlled by presenting heterogeneous affiliation centres (or even compositional assessing inside the MHP) for frequently modified charge partition and response movement, similar to the framework used in the field of photovoltaic daylight based cells. The HX corrosive, in any case, has priority over H O oxidation. Consequently, X3 should be diminished back to X utilizing extra decreasing specialists like H3PO2, which at last lessens the response's additional worth (Xu et al., 2017). Furthermore, HX's high corrosiveness will restrict the determination of some cocatalysts that are unsound in conditions like these.

Table 1: Utilizing MHP-based frameworks, a synopsis of revealed photocatalytic hydrogen age movement from haloacid (HX) arrangement has been accounted for.

Photocatalyst	**Solution**	**light source**	**Action (μmol/g/h)**	**Estimated time for stability (h)**
MAPbI3	Solution for HI	Light to be visible (470 nm ≤λ)	34	170
Pt/TiO2-MAPbI3	Solution for HI	Light to be visible (425 nm ≤λ), 200 mW/cm2	7400	13
MAPbI3/r GO	Solution for HI	Light to be visible (425 nm ≤λ), 300 W	949	210
Cs2AgBiBr6	Solution for HI	Light to be visible (425 nm ≤λ), 300 W	49.8	130
Black Phosphorus/MAPbI3	Solution for HI	Light to be visible (425 nm ≤λ), 300 mW/cm2	3572	210
PEDOT:PSS/MAPbBr3/Ta2O5	Solution for HI	Light to be visible (425 nm ≤λ), 150 mW/cm2	660	5
MAPbBr3−xIx/Pt	Mix solution for	Light to be visible (425 nm	2704.7	60

	HBr/HI	≤λ), 300 W		
CsPbBr3−xIx/Pt	Mix solution for HBr/HI	Light to be visible (425 nm≤ λ), 300 W	1220	60

3.3 Solvents with Low Polarity to Reduce CO2:

Because of the MHPs' ionic person, which renders them especially powerless against polar atom debasement, low-extremity solvents can be utilized to lay out hearty photocatalytic response conditions. Under ecological circumstances, the MHP precious stone doesn't promptly arrange with the dissolvable's relatively feeble dipole second, keeping them from being isolated into buildings of the creating ionic species. All-inorganic quantum dots (QDs) were used in this system by Kuang et al. and Sun et al. for photocatalytic CO2 reduction.; pay regard that this procedure moreover works with MHP nanocrystals and QDs. In Sun's review, ethyl acetic acid derivation was the low-extremity dissolvable joined with minute measures of water as opening scroungers (volume proportion: 300:1) (see Figure4A). Following 8 hours of reenacting sun based light openness, 35, 13, and 0.9 mol/g of CO, CH4, and H2 were created, separately. It ought to be noticed that water fills in as an oxygen generator by rummaging openings, however that water parting into hydrogen additionally represses the CO2 decrease cycle. The accompanying conditions (3-4) address the response processes:

$$2H_2O \rightarrow O_2 + 4H^- + 4e^- \qquad (3)$$

$$CO_2 + 2e^- + 2H^+ \rightarrow CO + H_2O \qquad (4)$$

Arrangement, X fills in as a penance, and X's oXidation to under these conditions, the CsPbBr3 QDs showed great primary soundness and saved their translucent design and surface shape (Xu et al., 2018). As shown in Figure 4B, the CsPbBr3 QDs were changed by the addition of graphene oxide (GO), which is ideal for useful electron extraction and transport. (Poli et al., 2017). As per Figure 4C, the made CsPbBr3/GO composite showed an around 25% higher electron utilization rating (357.4 mol/g) than the first CsPbBr3 material (284.7 mol/g). In the last option case, the response media was unadulterated ethyl acetic acid derivation without the expansion of water. Vulnerability encompasses the attributes of the framework's opening forager.

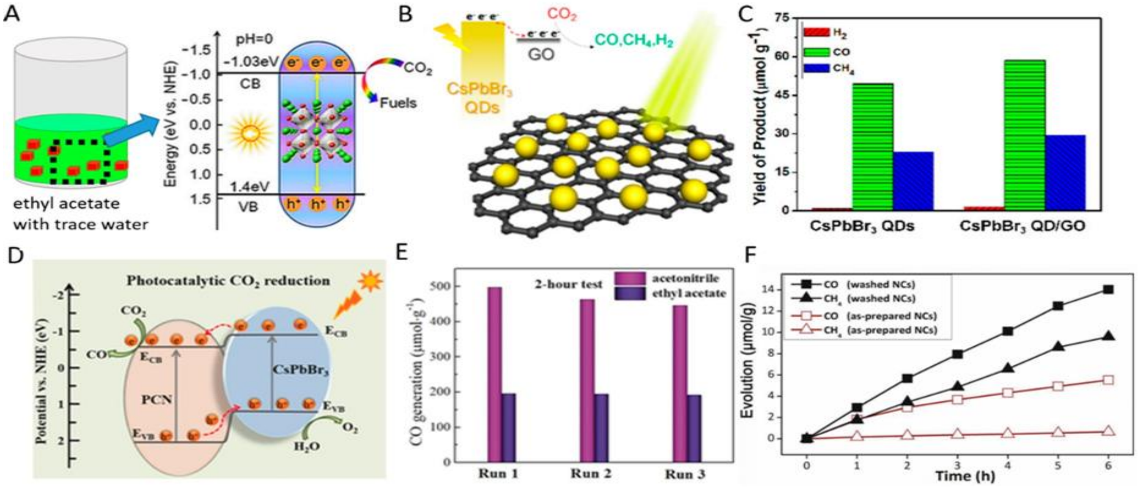

Figure 4: Utilization of CsPbBr3

CsPbBr3 is utilized in (A) to lessen CO2 through photocatalysis in a 300/1 ethyl acetic acid derivation/water mix. (B) For photocatalytic CO2 reduction in ethyl acidic corrosive determination, the CsPbBr3 and graphene oxide reaction plot, and (C) the thing yield in this structure. (D) A band diagram of the CO generation for three consecutive runs of two hours each using the CsPbBr3 QDs/g-C3N4 composite photocatalyst in the acetonitrile/water and ethyl acidic destructive allowance/water structures. (F) The sustained rise in CO and CH4 resulting from the CO2 reduction brought on by Cs2AgBiBr6 NCs in the ethyl acidic corrosive equation.

3.4 Encapsulation:

A major modification approach is to enclose the MHP in a protective layer inside center shell particles. Direct relationship between the MHP and undermining polar particles is stayed away from by the cutoff. It is basic to look out that the MHP isn't kept away from getting light by the shell material. Kuang and accessories made CsPbBr3@TiO2 center shell structures involving dubious TiO2 as the encasing material. Figure 5 shows the TEM image of this centre shell structure with the CsPbBr3 nanocrystal covered in hazy TiO2 (Poli, et al., 2019). Due to prolonged electron transfer from CsPbBr3 to TiO2, with more pronounced improvement than revealed CsPbBr3, this photocatalyst was utilized to lessen CO2 in ethyl acidic destructive derivation/water under sun organized light enlightenment. The way that this center shell improvement holds more than 90% of its covered up photocatalytic advancement following 15 unique times is essential. The encased material kept on having basically undefined photocatalytic advancement regardless, following 30 hours of steady reenactment of sun arranged light enlightenment, as tended to in Figure 6B. Wu et al. all things considered utilized vulnerable graphitic carbon nitride (p-g-C3N4) to cover CsPbBr3 microparticles and involved it to speed up malachite green debasement in polar isopropanol. As p-g-C3N4 endeavored to defend the CsPbBr3 surface, this stimulus saved a consistent activity for 10 cycles (or generally 4.7 hours). It has likewise been shown that the center shell structure helps with balancing out the MHP in high-extremity solvents, for example, water notwithstanding low-extremity solvents (Al-Dosar & Abdellatif, 2024; Bagga et al., 2014; Kumar et al., 2023; Kim & AlZubi, 2024).

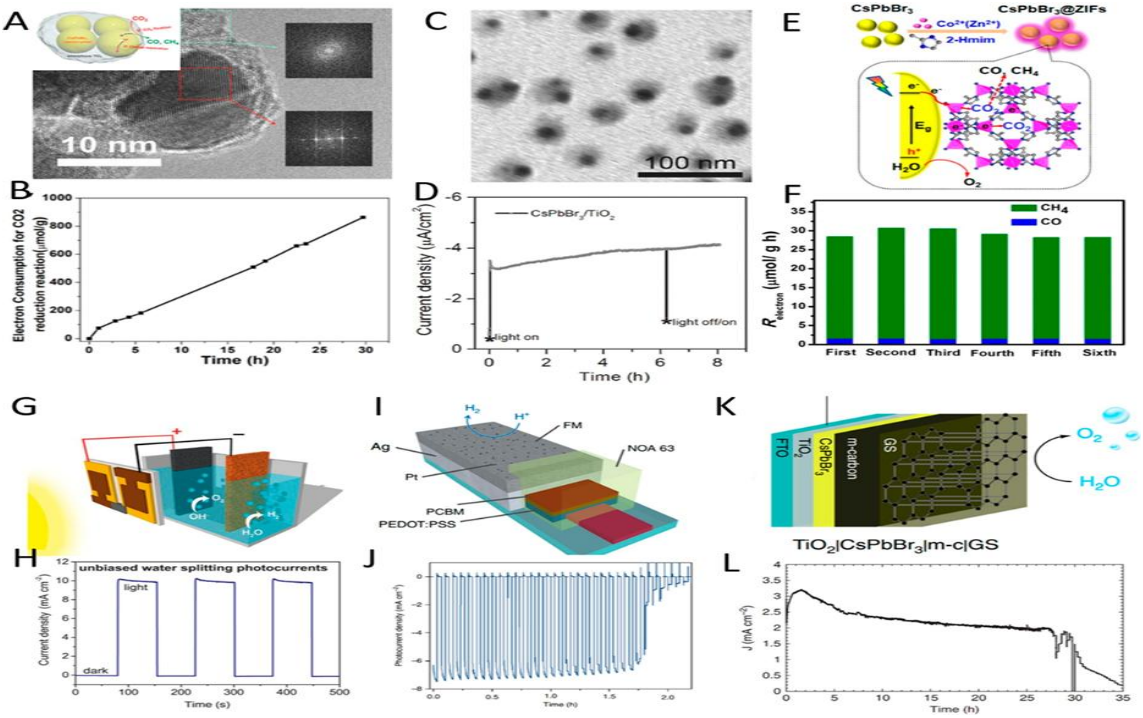

Figure 5: Encapsulation

In figure (A) TEM photos of a shapeless TiO2-exemplified CsPbBr3 nanocrystal, and (B) a period pass of the photocatalytic CO2 decrease of isopropanol follows in ethyl acetic acid derivation affected by sun oriented light. The CsPbBr3/TiO2 NCs terminal went through controlled expected electrolysis in unbiased water in somewhere around 8 hours, as displayed in (C) TEM pictures of anatase TiO2-covered center/shell NCs and (D). The diagrams in (E) and (F), respectively, depict how CsPbBr3@ZIF-67 is made, how charges travel inside it, and how it is used to reduce CO2 in ethyl acetic acid synthesis setups. When exposed to solar radiation without any outside influence, the device's momentum thickness time bends (G) in a solar-powered Perovskite water-parting cell and (H). The strength of the photocathode is assessed using a light-slashed chronoamperometry test in (I) the design sketch of the FTO/PEDOT: PSS/perovskite/PCBM/PEIE: Ag photocathode for water reduction. (K) Additionally, soundness (L) for water oxidation with sun-directed light illumination has been drawn out (Min et al., 2024; Riad et al., 2024; Rolla, 2023).

RESULTS

4.1 Realizing MHP Stability from Within:

While the aforementioned methodologies provide varying degrees of progress under somewhat controlled circumstances, they fall short of providing a path toward global gathering. The trickiness of the MHPs when applied to situations that would typically be responsive is what led to this error, as has been emphasized throughout. Clearly, the really clever strategy is to support MHPs that can naturally overcome typical photocatalytic circumstances and, more importantly, exhibit long-term photocatalytic performance. All-inorganic perovskites are more stable than hybrid regular inorganic perovskites due to their higher course of action energy, lower configurational entropy, lack of brittleness, and reduced hygroscopic nature. The use of some entirely inorganic perovskites in water-rage-based reactions has been productive. Kuang et al. created the CsPbBr3/BZNW/MRGO composite for the photo reactant abatement of CO2 inside seething water. The framework was initially created using a combination of CsPbBr3 NC and MRGO (macroporous graphene oxide). The development of ZnO nanowires increased both the photoelectron utilization rate with the CsPbBr3 NCs in their most ideal configuration and the CsPbBr3/MRGO to >50 mol/g/h. Furthermore, the CH4 age stayed consistent during the course of 4 cycles, or 16 hours, of repeated daylight-based lighting up, without displaying any signs of lowering. Kuang then looked at the dependability of MHP photocatalysts without lead when used with polar particles. Rb3Bi2I9, Cs3Bi2I9, and MA3Bi2I9 were produced in a similar manner using a progressive ultrasonication cycle to produce materials that can sustain consciousness for seven days in a setting with 70% moisture. After that, these perovskites and water smoulder were used to reduce the CO2. As seen in Figure 6A, a number of center species, such as anion length carbonate, monodentate carbonate, and bidentate carbonate, can develop when CO2 and H2O are adsorbed on the perovskite surface. Figure 6B illustrates how CH4 on these perovskites improved over time as the amount of light increased. Over the course of 10 hours, CH4 production steadily rises. More surprisingly, Navas developed smaller-than-normal CsSnBr3 particles in 2018 for the photocatalytic variety degradation in watery game theory. Because the hydroXyl progressives sent by the CsSnBr3 VB (1.9 eV vs RHE) are more certain than the Benevolent/•OH redoX potential, the violet tone was removed as seen in Figure 6C. Figure 6D shows that during five cycles (15 straight hours) of photoactivity in a liquid game plan containing 2.0 mg/L of precious stone violet tone, there was no compromise.

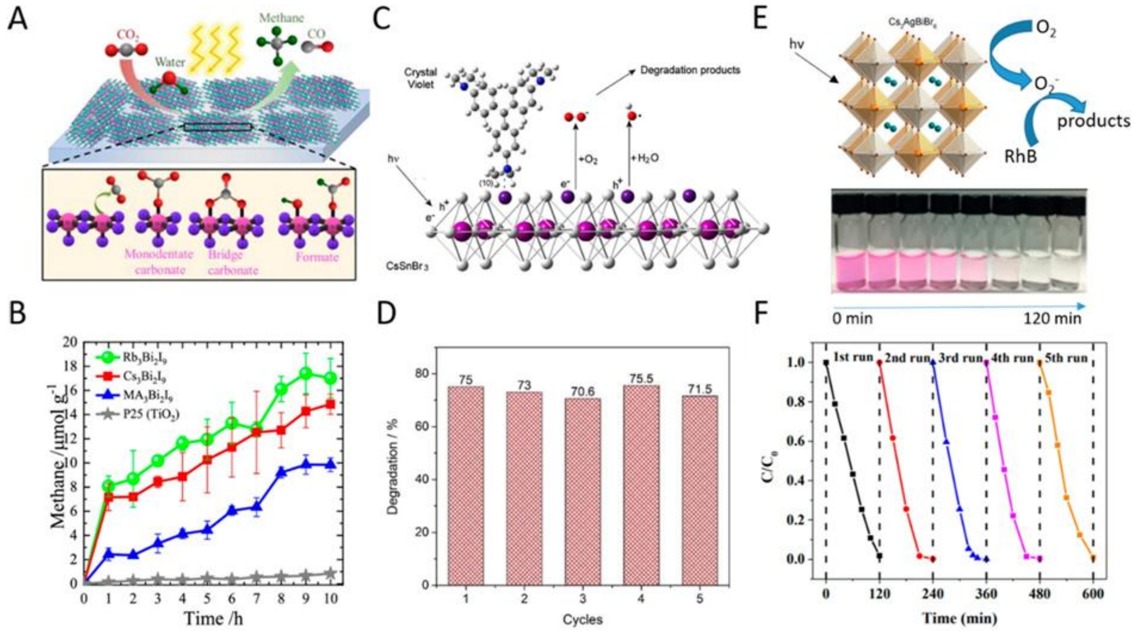

Figure 6: Realizing Intrinsic MHP Stability

However, for steady operation in alcohols, researchers have also looked into all-inorganic MHP photocatalysts. To assist the breakdown of the anti-toxin antibiotic drug hydrochloride (TC-HCl) in ethanol, Fan et al. created CsPbBr3 nanoparticles. In a short time subsequent to being presented to noticeable light, 76% of TC-HCl could be separated. $CsPbBr_3$ kept on displaying more than 90% of its unique action after 4 rounds of examinations enduring a sum of 120 min. The fractional action misfortune is a consequence of photocatalyst material being lost during recuperation between cycles. Xu et al. demonstrated $Cs_2AgBiBr_6$ microparticles appropriate for photocatalytic response in ethanol, depending on the material's significantly expanded synthetic robustness.100 In Figure 6E, under ceaseless light, ca. In the span of two hours, the $Cs_2AgBiBr_6$ photocatalyst annihilated 98% of Rhodamine B (RhB). The principal species engaged with the breakdown of RhB in this response is created really by superoxide revolutionaries. Following 6 hours (5 patterns) of illumination, the material, as displayed in Figure 7F, kept up with its photoactivity and that amount dependability in ethanol, but a limited quantity of AgBr created as water particles might make the $Cs_2AgBiBr_6$ precious stone to some extent disintegrate. Epoxides were absorbed and activated by Lewis damaging Bi complaints in $Cs_3Bi_2Br_9$. Alcohols and O_2 interacted with light-enacted apertures and electrons in $Cs_3Bi_2Br_9$ to deliver separate alcohol anions and superoxide devotees. Liquor anions act as nucleophiles. and liquor revolutionaries created by the response of superoXide extremists with alcohols would respond with initiated epoxides to make ether. Following 6 hours of apparent light openness, $Cs_3Bi_2Br_9$ changed the vast majority of the styrene oxide. Furthermore, $Cs_3Bi_2Br_9$ kept on showing a decent movement (holding 80% of its underlying photocatalytic action) following three cycles (18 hours altogether).

4.2. Increasing MHPs' operational stability and long-term catalytic cycling:

While various responses have been effectively completed in radiance corrosive and low-extremity arrangements, these strategies are not commonly relevant. Restricting contact between the MHPs and any polar dissolvable will help to expand protection from material debasement pathways by making center shell structures, (for example, oxide covering layers) with almost amazing inclusion. There were plans for sturdy contraption buildings. Therefore, using top and bottom HTL and ETL materials to completely cover MHPs by turn covering, CVD, or ALD provides a path that may be able to pass MHP photocatalysts that are steady on for a prolonged period of time. HTL and ETL would also contribute to the separation and relocation of charge transporters in MHPs. An even more predictable perovskite arrangement may be achieved by raising the valence charges of the dopant particles to enhance the bond between the particles and the important stone edge without the need for extra functionalization. For sunlight-based cells, LEDs, and other optoelectronic devices, it has been intensively examined if it is possible to partially or entirely substitute the Pb in MHP with alternative metals. A similar compositional change can increase the availability of MHP devices without materially compromising optoelectronic performance. It is immensely humble to consider the possibility of further research into this strategy for photocatalytic applications. By controlling the lead hydroxide exterior layer in octahedral perovskite math under both acidic and focal media at enclosed settings, continuous testing has shown that the perovskite microstructure may be stable decreased for more than six months. Under neutral, acidic, and essential conditions, the sun-based water isolating limitations of these water-stable perovskites can be clearly seen. Once they have separated from traditional photocatalysts like TiO_2 and perovskite oxides ABO, MHP-based photocatalysts have the ability to significantly increase their power and future.

4.3. Increasing the efficiency of CO_2 reduction and H_2 synthesis on photocatalysts based on MHP:

There are several reasonable ways to deal with working with work on the movement of MHPs photocatalysis for H_2 blend and CO_2 decline, including the expansion of co-impetuses (Pt, Au, Ag, CoO, MoS_2, and so on) to accelerate the pace of surface responses, the union of nanostructure morphologies with additional uncovered surfaces, (for example, nanosheets and nanoplatelets), and the development of novel heterojunctions to further develop charge detachment.

4.4. Increasing the MHP-based photocatalysis' redox capacity:

Powerless redoX capacities and, explicitly corresponding to the VB edge, feeble oXidation capacities will certainty result from the similarly restricted bandgaps of MHPs. The restriction of the little bandgap MHP to oxidate will be endeavored by unambiguous oXidation processes, notably the oXidation of water and the irrational mineralization of conventional compounds. Making a heterostructure by joining various semiconductors with a more reliable VB is an optional method of delivering broad light support and a strong redoX limit (making a Z-arrangement). Naturally, the applied voltage can also cultivate the redoX furthest reaches of the MHP to achieve a broad response scope by building the MHP-based PEC response framework.

CONCLUSION

Generally, in view of the conversation above, it tends to be presumed that MHP film frameworks, which incorporate MHP sun based cells combined with electrocatalyst and photoelectrocatalyst as well as defensive layers totally covering to shape a MHP photoelectrode, accomplish "consistent" PEC energy change in fluid circumstances. In these frameworks, MHP was isolated from the fluid arrangement and utilized as a light collector to take in sun based light and produce transporters. Therefore, MHP's solidness would be altogether expanded. Halide perovskites in watery arrangements can effectively utilize sunlight based energy by utilizing these PEC frameworks.

There are various indisputable optoelectronic applications for MHP semiconductors because of their excellent optical qualities (i.e., sun powered cells, LEDs, photodetectors, and so on.). MHPs were as of late reused for photograph synergist processes and sunlight based to-compound energy transformation because of their interesting photophysics. Nonetheless, a critical specialized challenge is presented by the ionic precious stone design's normally low security. Their instability has substantially limited the range of heterogeneous photocatalytic responses that MHPs can be used to, which has prompted examination into systems to defeat it.

We have evaluated the most recent upgrades in this review, the area of MHP-based photocatalysis, zeroing in on the shakiness gives that are correct now blocking development. A couple "stable" MHP-based photocatalytic structures, including H2 age from doused brilliance destructive plans, CO2 diminishing and regular blend in low-furthest point solvents, CO2 decreasing and variety debasement exemplification and covering of MHPs for CO2 decrease and photoelectrochemical water separating on all-inorganic MHPs with sensible polar solvents, have been planned and acknowledged to conquer material hazards. Potential outcomes to make imaginative composite perovskites with further developed precious stone dependability have additionally been shown. There are various promising courses for upgrading the security and adequacy of MHP-based photocatalysis, contingent upon the current getting it and material limitations.

Acknowledgement

Funding Details

This work was supported by Dongseo University, "Dongseo Cluster Project (type 1)" Research Fund of 20240006

Authors' contributions

All authors contributed toward data analysis, drafting and revising the paper and agreed to be responsible for all the aspects of this work.

Declaration of Conflicts of Interests

Authors declare that they have no conflict of interest.

Availability of data and materials

Not Applicable

Use of Artificial Intelligence

Not applicable

Declarations

Authors declare that all works are original and this manuscript has not been published in any other journal.

REFERENCES

[1] Al-Dosari, M. N. A., & Abdellatif, M. S. (2024). The environmental awareness level among Saudi women and its relationship to sustainable thinking. Acta Innovations, 52, 28–42. https://doi.org/10.62441/ActaInnovations.52.4

[2] Bagga, T., Ansari, A. H., Akhter, S., Mittal, A., & Mittal, A. (2024). Understanding Indian consumers' propensity to purchase electric vehicles: An analysis of determining factors in environmentally sustainable

transportation. International Journal of Environmental Science, 10(1), 1–13. https://www.theaspd.com/resources/1.%20Electric%20Vehicles%20and%20Enviorment.pdf

[3] Brenner, T. M., Egger, D. A., Kronik, L., Hodes, G., & Cahen, D. (2016). Hybrid organic-inorganic perovskites: Low-cost semiconductors with intriguing charge-transport properties. Nature Reviews Materials, 1, 15007.

[4] Christians, J. A., Miranda Herrera, P. A., & Kamat, P. V. (2015). Transformation of the excited state and photovoltaic efficiency of CH3NH3PbI3 perovskite upon controlled exposure to humidified air. Journal of the American Chemical Society, 137, 1530–1538. https://doi.org/10.1021/jacs.5b11588

[5] Dong, Q., Fang, Y., Shao, Y., Mulligan, P., Qiu, J., Cao, L., & Huang, J. (2015). Science, 347(6225), 967–970. https://doi.org/10.1126/science.aaa5760.

[6] Elumalai, N. K., Mahmud, M. A., Wang, D., & Uddin, A. (2016). Perovskite solar cells: progress and advancements. Energies, 9(10), 861.

[7] Fujishima, A., & Honda, K. (1972). Electrochemical photolysis of water at a semiconductor electrode. Nature, 238(5358), 37-38.

[8] Ge, M., Li, Q., Cao, C., Huang, J., Li, S., Zhang, S., Chen, Z., Zhang, K., Al-Deyab, S. S., & Lai, Y. (2017). One-dimensional TiO2 nanotube photocatalysts for solar water splitting. Advanced Science, 4(6), 1600152.

[9] Giorgi, G., Fujisawa, J.-I., Segawa, H., & Yamashita, K. (2013). Journal of Physical Chemistry Letters, 4(23), 4213–4216.

[10] Green, M. A., Ho-Baillie, A., & Snaith, H. J. (2014). Nature Photonics, 8, 506–514.

[11] Guo, L., Chen, Y., Su, J., Liu, M., & Liu, Y. (2019). Energy, 172, 1079–1086. https://doi.org/10.1016/j.energy.2019.02.016.

[12] Ha, S.-T., Su, R., Xing, J., Zhang, Q., & Xiong, Q. (2017). Metal halide perovskite nanomaterials: Synthesis and applications. Chemical Science, 8(4), 2522–2536.

[13] He, R. A., Cao, S., Zhou, P., & Yu, J. (2014). Recent advances in visible light Bi-based photocatalysts. Chinese Journal of Catalysis, 35(6), 989–1007.

[14] Hendon, C. H., Tiana, D., Fontecave, M., Sanchez, C., D'arras, L., Sassoye, C., Rozes, L., Mellot-Draznieks, C., & Walsh, A. (2013). Engineering the optical response of the titanium-MIL-125 metal-organic framework through ligand functionalization. Journal of the American Chemical Society, 135(29), 10942-10945.

[15] Herz, L. M. (2016). Charge-carrier dynamics in organic-inorganic metal halide perovskites. Annual Review of Physical Chemistry, 67, 65–89.

[16] Hisatomi, T., Kubota, J., & Domen, K. (2014). Understanding TiO2 photocatalysis: mechanisms and materials. Chemical Society Reviews, 43(22), 7520-7535.

[17] Hou, J., Cao, S., Wu, Y., Gao, Z., Liang, F., Sun, Y., Lin, Z., & Sun, L. (2017). Inorganic colloidal perovskite quantum dots for robust solar CO2 reduction. Chemistry - A European Journal, 23, 9481–9485. https://doi.org/10.1002/chem.201701162.

[18] Huang, J. B., Tan, S. Q., Lund, P. D., & Zhou, H. P. (2017). Impact of H2O on organic-inorganic hybrid perovskite solar cells. Energy & Environmental Science, 10, 2284–2311. https://doi.org/10.1039/C7EE01334F.

[19] Jiang, Y., Cho, S.-Y., & Shim, M. (2018). Light-emitting diodes of colloidal quantum dots and nanorod heterostructures for future emissive displays. Journal of Materials Chemistry C, 6(10), 2618-2634.

[20] Jin, H., Debroye, E., Keshavarz, M., Scheblykin, I. G., Roeffaers, M. B. J., Hofkens, J., & Steele, J. A. (2020). It's a trap! On the nature of localized states and charge trapping in lead halide perovskites. Materials Horizons, 7(2), 397–410.

[21] Kamat, P. V. (2007). Meeting the clean energy demand: nanostructure architectures for solar energy conversion. The Journal of Physical Chemistry C, 111(7), 2834-2860.

[22] Kibria, M. G., & Mi, Z. (2016). Artificial photosynthesis using metal/nonmetal-nitride semiconductors: current status, prospects, and challenges. Journal of Materials Chemistry A, 4(8), 2801-2820.

[23] Kim, D., Sakimoto, K. K., Hong, D., & Yang, P. (2015). Artificial photosynthesis for sustainable fuel and chemical production. Angewandte Chemie International Edition, 54(11), 3259-3266.

[24] Kim, T. H., & AlZubi, A. A. (2024). AI enhanced precision irrigation in legume farming: Optimizing water use efficiency. Legume Research. https://doi.org/10.18805/LRF-791

[25] Kong, D., Zheng, Y., Kobielusz, M., Wang, Y., Bai, Z., Macyk, W., Wang, X., & Tang, J. (2018). Recent advances in visible light-driven water oxidation and reduction in suspension systems. Materials Today, 21(8), 897-924.

[26] Kumar, V., Chaturvedi, V., Lal, B., & Alam, S. (2023). Application of machine learning in analyzing the psychological well-being among the employees in the private sector: An analysis of work-life balance in the healthcare industry. Pacific Business Review International, 16(1), 124–131.

[27] Kwon, Y. S., Lim, J., Yun, H.-J., Kim, Y.-H., & Park, T. (2014). A diketopyrrolopyrrole-containing hole transporting conjugated polymer for use in efficient stable organic-inorganic hybrid solar cells based on a perovskite. Energy & Environmental Science, 7, 1454–1460. https://doi.org/10.1039/C3EE43935B.

[28] Lee, M. M., Teuscher, J., Miyasaka, T., Murakami, T. N., & Snaith, H. J. (2012). Efficient hybrid solar cells based on meso-superstructured organometal halide perovskites. Science, 338(6107), 643–647. https://doi.org/10.1126/science.1228604.

[29] Li, X., Yu, J., & Jaroniec, M. (2016). Hierarchical photocatalysts. Chemical Society Reviews, 45(8), 2603–2636.

[30] Lin, Q., Armin, A., Burn, P. L., & Meredith, P. (2016). Organohalide perovskites for solar energy conversion. Accounts of Chemical Research, 49(3), 545–553. https://doi.org/10.1021/acs.accounts.5b00483.

[31] Min, P. K., Mito, K., & Kim, T. H. (2024). The evolving landscape of artificial intelligence applications in animal health. Indian Journal of Animal Research. https://doi.org/10.18805/IJAR.BF-1742.

[32] Mosconi, E., Amat, A., Nazeeruddin, M. K., Grätzel, M., & De Angelis, F. (2013). First-principles modeling of mixed halide organometal perovskites for photovoltaic applications. Journal of Physical Chemistry C, 117(27), 13902–13913.

[33] Mosconi, E., Azpiroz, J. M., & De Angelis, F. (2015). Ab initio molecular dynamics simulations of methylammonium lead iodide perovskite degradation by water. Chemistry of Materials, 27, 4885–4892. https://doi.org/10.1021/acs.chemmater.5b01347.

[34] Murali, B., Dey, S., Abdelhady, A. L., Peng, W., Alarousu, E., Kirmani, A. R., Cho, N., Sarmah, S. P., Parida, M. R., Saidaminov, M. I., Zhumekenov, A. A., Sun, J., Alias, M. S., Yengel, E., Ooi, B. S., Amassian, A., Bakr, O. M., & Mohammed, O. F. (2016). Surface restructuring of hybrid perovskite crystals. ACS Energy Letters, 1(6), 1119–1126.

[35] Park, N.-G., & Segawa, H. (2018). ACS Photonics, 5, 2970–2977. https://doi.org/10.1021/acsphotonics.8b00792.

[36] Park, S., Chang, W. J., Lee, C. W., Park, S., Ahn, H. Y., & Nam, K. T. (2017). Photocatalytic hydrogen generation from hydriodic acid using methylammonium lead iodide in dynamic equilibrium with aqueous solution. Nature Energy, 2, 16185.

[37] Poli, I., Hintermair, U., Regue, M., Kumar, S., Sackville, E. V., Baker, J., Watson, T. M., Eslava, S., & Cameron, P. J. (2019). Graphite-protected CsPbBr3 perovskite photoanodes functionalised with water oxidation catalyst for oxygen evolution in water. Nature Communications, 10, 2097. https://doi.org/10.1038/s41467-019-10035-4.

[38] Qian, R., Zong, H., Schneider, J., Zhou, G., Zhao, T., Li, Y., Yang, J., Bahnemann, D. W., & Pan, J. H. (2019). Charge carrier trapping, recombination, and transfer during TiO2 photocatalysis: An overview. Catalysis Today, 335, 78–90. https://doi.org/10.1016/j.cattod.2018.10.053.

[39] Quan, L. N., García de Arquer, F. P., Sabatini, R. P., & Sargent, E. H. (2018). Metal-halide perovskites for photovoltaic and light-emitting devices. Advanced Materials, 30, 1801996.

[40] Quilettes, D. W. D., Vorpahl, S. M., Stranks, S. D., Nagaoka, H., Eperon, G. E., Ziffer, M. E., Snaith, H. J., & Ginger, D. S. (2015). Science, 348(6240), 683–686.

[41] Riad, A., Ben Zohra, M., & Alhamany, A. (2024). The enhancing PV stations for charging electric vehicles by utilizing shape memory alloy to track the sun and decrease fatigue. Metallurgy and Materials Engineering, 30(2), 12–24. https://doi.org/10.56801/MME1040.

[42] Rolla, K. J. (2023). Trends and futuristic applications of big data and electronic health record data in empowering constructive clinical decision support systems. Bio-Science Research Bulletin, 39(2), 78–91.

[43] Schneider, J., & Bahnemann, D. W. (2013). Undesired role of sacrificial reagents in photocatalysis. Journal of Physical Chemistry Letters, 4, 3479–3483. https://doi.org/10.1021/jz402055h.

[44] Stranks, S. D., & Snaith, H. J. (2015). Metal-halide perovskites for photovoltaic and light-emitting devices. Nature Nanotechnology, 10(5), 391–402.

[45] Suarez, B., Gonzalez-Pedro, V., Ripolles, T. S., Sanchez, R. S., Otero, L., & Mora-Sero, I. (2014). Journal of Physical Chemistry Letters, 5, 1628–1635.

[46] Takata, T., & Domen, K. (2019). Particulate photocatalysts for water splitting: Recent advances and prospects. ACS Energy Letters, 4(2), 542–549. https://doi.org/10.1021/acsenergylett.8b02209

[47] Tamirat, A. G., Rick, J., Dubale, A. A., Su, W.-N., & Hwang, B.-J. (2016). Using hematite for photoelectrochemical water splitting: a review of current progress and challenges. Nanoscale Horizons, 1(3), 243-267.

[48] Wang, D., Wright, M., Elumalai, N. K., & Uddin, A. (2016). Solar Energy Materials and Solar Cells, 147, 255–275.

[49] Wang, R., Mujahid, M., Duan, Y., Wang, Z.-K., Xue, J., & Yang, Y. (2019). A review of perovskite solar cell stability. Advanced Functional Materials, 29(47), 1808843.

[50] Wang, R., Mujahid, M., Duan, Y., Wang, Z.-K., Xue, J., & Yang, Y. (2019). A review of perovskites solar cell stability. Advanced Functional Materials, 29, 1808843.

[51] Wehrenfennig, C., Eperon, G. E., Johnston, M. B., Snaith, H. J., & Herz, L. M. (2014). High charge carrier mobilities and lifetimes in organolead trihalide perovskites. Advanced Materials, 26(10), 1584–1589.

[52] Wen, J., Xie, J., Chen, X., & Li, X. (2017). A review on g-C_3N_4-based photocatalysts. Applied Surface Science, 391, 72-123.

[53] Wu, Y., Chen, W., Chen, G., Liu, L., He, Z., & Liu, R. (2018). The impact of hybrid compositional film/structure on organic-inorganic perovskite solar cells. Nanomaterials, 8(5), 356.

[54] Wu, Y., Chen, W., Chen, G., Liu, L., He, Z., & Liu, R. (2018). The impact of hybrid compositional film/structure on organic-inorganic perovskite solar cells. Nanomaterials, 8(5), 356.

[55] Xiao, M., Wang, Z., Lyu, M., Luo, B., Wang, S., Liu, G., Cheng, H.-M., & Wang, L. (2019). Advanced Materials, 31(2), 1801369.

[56] Xiao, X., Jiang, J., & Zhang, L. (2013). Selective oxidation of benzyl alcohol into benzaldehyde over semiconductors under visible light: The case of Bi12O17Cl2 nanobelts. Applied Catalysis B: Environmental, 142-143, 487.

[57] Xie, S., Zhang, Q., Liu, G., & Wang, Y. (2016). Photocatalytic and photoelectrocatalytic reduction of CO2 using heterogeneous catalysts with controlled nanostructures. Chemical Communications, 52(1), 35-39.

[58] Xing, G., Mathews, N., Sun, S., Lim, S. S., Lam, Y. M., Grätzel, M., Mhaisalkar, S., & Sum, T. C. (2013). Long-range balanced electron- and hole-transport lengths in organic inorganic CH3NH3PbI3. Science, 342(6156), 344–347. https://doi.org/10.1126/science.1243167.

[59] Xu, Y. F., Yang, M. Z., Chen, B. X., Wang, X. D., Chen, H. Y., Kuang, D. B., & Su, C. Y. (2017). A CsPbBr3 perovskite quantum dot/graphene oxide composite for photocatalytic CO2 reduction. Journal of the American Chemical Society, 139, 5660–5663. https://doi.org/10.1021/jacs.7b00580.

[60] Xu, Y.-F., Wang, X.-D., Liao, J.-F., Chen, B.-X., Chen, H.-Y., & Kuang, D.-B. (2018). Amorphous-TiO2-encapsulated CsPbBr3 nanocrystal composite photocatalyst with enhanced charge separation and CO2 fixation. Advanced Materials Interfaces, 5, 1801015. https://doi.org/10.1002/admi.201801015.

[61] Yang, W. S., Noh, J. H., Jeon, N. J., Kim, Y. C., Ryu, S., Seo, J., & Seok, S. I. (2015). High-performance photovoltaic perovskite layers fabricated through intramolecular exchange. Science, 348(6240), 1234–1237.

[62] Zhou, H., Qu, Y., Zeid, T., & Duan, X. (2012). Towards highly efficient photocatalysts using semiconductor nanoarchitectures. Energy & Environmental Science, 5, 6732–6743. https://doi.org/10.1039/C2EE21486B.

[63] Zhou, P., et al. (2021). Nature Communications, 12, 4412. https://doi.org/10.1038/s41467-021-24619-3

[64] Zhu, Z., Hadjiev, V. G., Rong, Y., Guo, R., Cao, B., Tang, Z., Qin, F., Li, Y., Wang, Y., Hao, F., Venkatesan, S., Li, W., Baldelli, S., Guloy, A. M., Fang, H., Hu, Y., Yao, Y., Wang, Z., Bao, J. (2016). Interaction of organic cation with water molecule in perovskite MAPbI3: From dynamic orientational disorder to hydrogen bonding. Chemistry of Materials, 28(20), 7385–7393.